*Journal of Applied Electrochemistry* **30**: 209–216, 2000.



# Study of mixing in an axisymmetric coflowing liquid jet by coupling L.D.A. to an electrochemical method

S. BENAYAD[1], A. SALEM[2] and J. LEGRAND[3]*
[1] *Institut Algérien du Pétrole, Boumerdes 35000, Algeria*
[2] *Laboratoire de Mécanique des Fluides, Institut de Physique, USTHB, Bab Ezzouar, Algeria*
[3] *Laboratoire de Génie des Procédés-UPRES EA 1152, CRTT, IUT-BP406, 44602 Saint Nazaire, France*
*(*author for correspondence, e-mail: jack.legrand@lgp.univ-nantes.fr; fax: +33 2 4017 2618)*

Received 8 January 1999; accepted in revised form 18 August 1999

*Key words:* jet, L.D.A., mixing, polarography, turbulence

**Abstract**

Local and simultaneous velocity and concentration fluctuations were analysed in an axisymmetric jet of an aqueous electrolyte solution moving in a codirectional water stream. The determination of the convection velocity of the turbulent eddies as well as correlation between axial velocity and concentration fluctuations was made possible by coupling L.D.A. to an electrochemical technique. The influence of the ratio of the coflowing stream velocity to the jet exit velocity was investigated. The mean velocity and concentration profiles, the turbulence intensity, the integral length scales relative to axial velocity and concentration were also determined.

**List of symbols**

| | |
|---|---|
| $a$, $b$ | constants |
| $C(t)$ | instantaneous concentration (mol m$^{-3}$) |
| $c(t)$ | concentration fluctuations (mol m$^{-3}$) |
| $d$ | injector diameter (cm) |
| $D$ | molecular diffusion coefficient (m$^2$ s$^{-1}$) |
| $D_t$ | momentum turbulent diffusion coefficient (m$^2$ s$^{-1}$) |
| $G$ | axial velocity, concentration or temperature |
| $h$ | half value radius (m) |
| $I$ | electrical current ($\mu$A) |
| $K_E$ | Euler's correlation function for concentration |
| $L$ | integral scale (m) |
| $m$ | velocities ratio, $m = U_p/U_j$ |
| $r$ | radial coordinate (m) |
| $Re$ | Reynolds number, $Re = dU_j/v$ |
| $R_E$ | Eulerian time correlation for velocity |
| $R_{uc}$ | Axial velocity–concentration correlation coefficient |
| $R_{ut^\circ}$ | Velocity–temperature correlation coefficient |
| $S$ | voltage signal |
| $Sc$ | Schmidt number, $Sc = v/D$ |
| $t^\circ$ | temperature fluctuations (°C) |
| $t$ | time (s) |
| $U(t)$ | instantaneous axial velocity (m s$^{-1}$) |
| $u$ | axial velocity fluctuation (m s$^{-1}$) |
| $U_p$ | coflow mean velocity (m s$^{-1}$) |
| $U_j$ | jet exit mean velocity (m s$^{-1}$) |
| $v$ | radial velocity fluctuation (m s$^{-1}$) |
| $\overline{U}_a$ | axial mean velocity (m s$^{-1}$) |
| $V_c$ | convection velocity (m s$^{-1}$) |
| $X_o$ | abscissa of the virtual origin of the jet (m) |
| $X$ | axial coordinate of the measuring section (m) |

*Greek symbols*

| | |
|---|---|
| $\alpha$ | calibration constant |
| $v$ | kinematic viscosity (m$^2$ s$^{-1}$) |
| $v_t$ | scalar turbulent diffusion coefficient (m$^2$ s$^{-1}$) |
| $\delta$ | distance between L.D.A. and probe measuring volumes (mm) |
| $\tau$ | time delay (s) |

*Subscripts/Superscripts*

| | |
|---|---|
| a | axis |
| c | concentration |
| j | jet |
| L | L.D.A. |
| p | coflowing stream |
| pp | polarographic probe |
| r | radius |
| t | turbulent |
| u, v | respective axial or radial velocity fluctuations |
| $^*$ or $^-$, $\langle\rangle$ | respectively dimensionless or time average |

## 1. Introduction

The mixing of two fluids which takes place in the combustion chamber of a small engine as well as in chemical reactors has attracted much attention. The optimization of chemical reactor performance may be achieved through a deeper understanding of chemical kinetics and of the dynamic conditions which control the mixing of the reactant species.

Turbulent jets are of prime importance in the field of mixing and have been studied both theoretically and experimentally for many years. The axisymmetric jet has received particular attention [1, 2]. The characteristic parameters of this flow type are well known and recent publications have further focussed on particular aspects [3–11]. However, most of the literature concerning axisymmetric jets is devoted to the case of the jet flowing in a fluid at rest or in an identical phase coflowing fluid.

Very few data deal with velocity–concentration correlations which require continuous and simultaneous acquisition of velocity and concentration. To achieve this goal, Benayad et al. [12] in the case of an agitated vessel and Gatard [13] for two-dimensional jet have coupled microconductimetry and L.D.A. techniques. Lemoine et al. [9, 10] coupled L.D.A. and laser-induced fluorescence and measured the velocity–concentration correlation in a submerged free jet. Siragna [14] coupled L.D.A. with the polarographic method and obtained the axial velocity–concentration correlation in an axisymmetric jet. The same experimental method was used in the present work.

In the following literature review we have made a survey of work dealing with the radial and axial variation of mixing characteristic parameters and, more particularly, the velocity–concentration cross-correlations in coflowing jets.

### 1.1. *Radial variation*

Dimensionless quantities like $U^*$, $C^*$ or $T^*$ are very often used in the literature dealing with jet studies. Their definition is as follows: if $\overline{G}$ denotes the mean axial velocity or mean concentration or mean temperature, a dimensionless quantity may be defined as

$$G^* = \frac{\overline{G} - G_p}{\overline{G}_a - G_p} \tag{1}$$

which becomes

$$G_a^* = \frac{\overline{G}_a - G_p}{G_j - G_p} \tag{2}$$

on the jet axis (Figure 1). The dimensionless mean axial velocity profiles $U^*$ become self-similar when $X = 8d$ as for Tong and Warhaft [7] and for $X \geq 20d$ in other studies [3, 6, 15]. The dimensionless mean concentration $C^*$ or temperature $T^*$ profiles become self-similar for $X \geq 15d$ in further investigations [ 4, 7, 16]. From these data it can be asserted that the dimensionless mean profiles become self-similar beyond $20d$ and are well fitted by a gaussian curve [1, 6, 17]. The dimensionless mean temperature or mean concentration variations are more pronounced than those of mean axial velocity [11, 17]. According to Wygnanski and Fiedler [3], the axial velocity fluctuation profiles, given by

$$u^* = \frac{\sqrt{(\overline{u^2})}}{\overline{U}_a - U_p} \tag{3}$$

do not become self-similar below $40d$. Furthermore, $u^*$ tends to a limiting value far from the jet exit [3, 6, 7, 11, 14, 15]. On the onehand, concerning the radial velocity fluctuation $v$, Wygnanski and Fiedler [3] assess that $\sqrt{(\overline{v^2})}$ (r.m.s.) remains smaller than the axial velocity $\sqrt{(\overline{u^2})}$ (r.m.s.) up to $100d$. On the other hand, $v$-fluctuation profiles become self-similar only if $X \geq 70d$ [3].

### 1.2. *Axial variation*

The dimensionless mean parameters of a round jet exhibit a hyperbolic variation [3, 7, 15, 18, 19]. Similarly, both concentration and temperature r.m.s hyperbolically

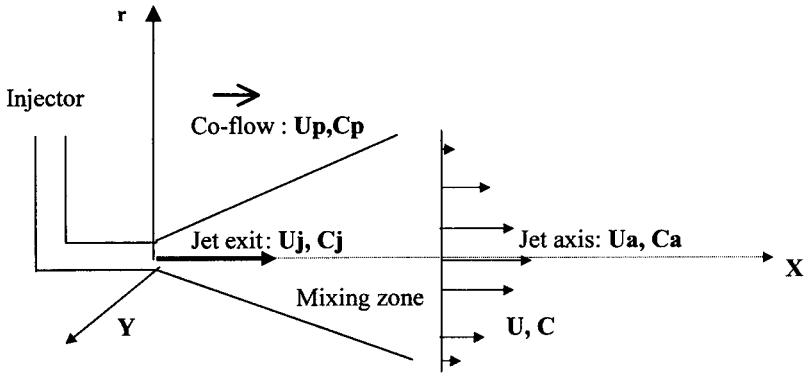


*Fig. 1.* Definitions of the quantities used.

decrease and tend to a limit value [4, 5, 7, 20]. Furthermore, the concentration profiles

$$c^* = \frac{\sqrt{(\overline{c^2})}}{\overline{C}_a - C_p} \tag{4}$$

normalized by the centerline values become larger with increasing Reynolds number [4]. Concerning the convection mean velocity of turbulent eddies $V_c$, only few investigations are available [3, 21, 22]. This parameter has been determined by Wygnanski and Fiedler [3] and compared with $\overline{U}$, the local mean axial velocity. They found $V_c/\overline{U} = 1.70$ on the jet edge and $V_c/\overline{U} = 0.90$ on the axis. Wu and Patterson [21] and Michelet et al. [22] have considered this parameter in the case of a jet induced by the impeller of a stirred tank reactor. These authors [21, 22] have reported that $V_c$ is greater than the local mean velocity. Michelet et al. [22] have further observed that this parameter decreases along the jet axis. These results are not in keeping with the generally accepted assumption of frozen turbulence $V_c/\overline{U} \simeq 1$.

The ratio of the coflowing stream velocity to the jet exit velocity $m = U_p/U_j$ plays an important role in the jet hydrodynamics as indicated by the results of Schetz [2]. Concerning the length scales and the cross-correlation coefficients, a linear increase with the abscissa $X$ [2, 3, 23] for the first parameters and the presence of well-marked maxima on both sides of the jet [3, 9, 11, 14, 24] for the second ones are the only results in perfect agreement with the literature. Otherwise, significant scatter is observed. For example, the microscale could vary by a factor of four according to the author [3, 15]. This scatter may be partly due variation in attention to signal treatment. Indeed, Chevray and Tutu [11] claim that 70% of $\overline{uv}$ energy and 50% of $\overline{ut^\circ}$ are contained within the frequency band 0–10 Hz for $X = 15d$. Moreover, Wygnanski and Fiedler [3] assert that neglecting the frequencies below 2 Hz induced a 27% error in the value of $\overline{u^2}$ and about 11% in that of $\overline{v^2}$. These authors [3] observe that filtering the frequencies below 3 Hz can modify the velocity microscale by 100%.

## 2. Experimental apparatus and measurement techniques

### 2.1. *Description of the experimental apparatus*

The experiments were carried out at controlled temperature in a PMMA channel. The working section was 320 cm long, 12 cm wide and 40 cm deep. The coflowing solution velocity $U_p$ was variable in the range 8–65 cm $s^{-1}$. An axisymmetric jet was formed by introducing a polarographic solution (potassium ferricyanide at 2.4 mol $m^{-3}$ and potassium ferrocyanide at 7.2 mol $m^{-3}$) through a round injector (Figure 2). The injector was continuously fed from a constant level supply tank. The tank level was adjustable and the jet exit velocity $U_j$ was variable between 0 and 140 cm $s^{-1}$. These velocities allow the ratio $m = U_p/U_j$ to be varied between 0.057 and infinity. The experimental conditions are listed in Table 1.

The polarographic method is based on electrochemical reaction under diffusion-control condition of a reactant solution in a moving liquid. At the limiting current, the concentration at the electrode surface is zero. Our probe is a hot wire-type device; it was made of

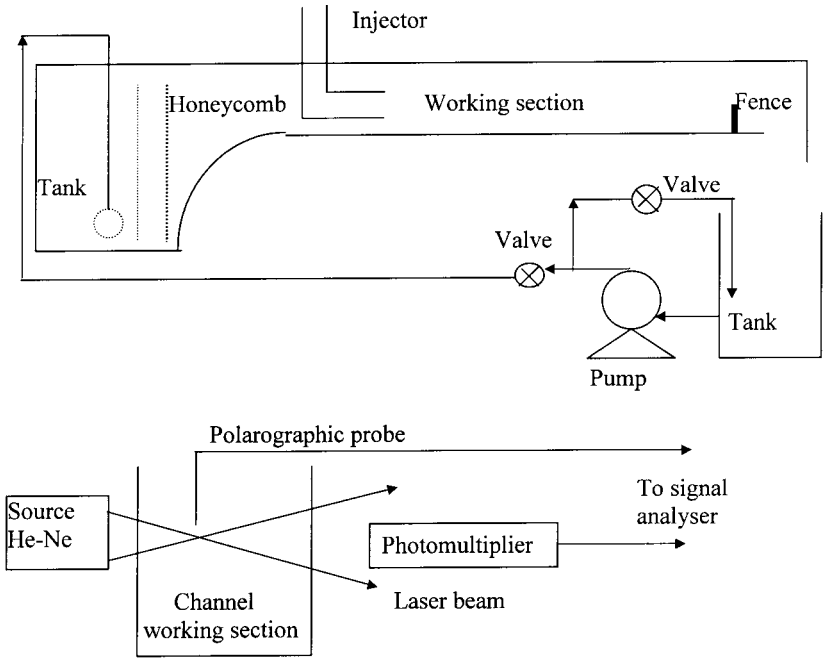


*Fig. 2.* Hydraulic circuit and measurement devices arrangement.

*Table 1.* Experimental conditions

| $U_p$/cm s$^{-1}$ | $U_j$/cm s$^{-1}$ | $m$ | $d$/cm | $X/d$ | $C_p$/mol m$^{-3}$ | $C_j$/mol m$^{-3}$ | D/cm$^2$ s$^{-1}$ | $Sc$ | $Re$ |
|---|---|---|---|---|---|---|---|---|---|
| 12 | 97 | 0.12 | 0.32 | 20 or 30 | 1 | 1 | $9.218 \times 10^{-6}$ | 943 | 3572 |
| 12.4 | 114 | 0.11 | 0.20 | 51 or 57 | 1 | 2.4 | $7.129 \times 10^{-6}$ | 1431 | 2235 |
| 19.8 | 84 | 0.24 | 0.32 | 25 | | | | | 3002 |
| 23.7 | 84 | 0.28 | 0.32 | 25 | | | | | 3002 |
| 31 | 84 | 0.37 | 0.32 | 25 | | | | | 3002 |

a platinum wire 30 $\mu$m in diameter stretched between metallic pins, the platimum wire was insulated except the central portion which was 1.5 mm long and constitutes the sensitive element of the probe. If the concentration is constant and a large excess of a supporting electrolyte (KCl at 300 mol m$^{-3}$) is present, the probe delivers an electrical current proportional to the square root of the instantaneous fluid velocity [24]:

$$I = b_1 + a_1\sqrt{U(t)} \tag{5}$$

If the concentration $C$ varies with time, the current may be written as

$$I = \frac{C}{C_p}\left(b_1 + a_1\sqrt{U(t)}\right) \tag{6}$$

where $a_1$ and $b_1$ are two constants obtained by calibrating the probe in a solution with a concentration $C_p$. (In our experimental conditions: $a_1 = 0.98$ $\mu$A (s cm$^{-1}$)$^{1/2}$, $b_1 = -0.60$ $\mu$A and $C_p = 1$ mol m$^{-3}$).

The instantaneous velocities were measured by L.D.A. following the procedure described by Durst and Whitelaw [25]. Two laser beams from the same source are focused at a point of the flow where they form interference fringes. A photomultiplier detects the intensity fluctuations resulting from the passage of small solid impurities in the fluid stream. The L.D.A. system is equipped with a Bragg cell that gives the flow direction.

The current $I(t)$ from the polarographic probe is amplified and converted into a voltage:

$$S_{pp}(t) = \left(a\sqrt{U(t)} + b\right)\frac{C(t)}{C_p} \tag{7}$$

Also, the frequency tracker of the L.D.A. delivers an analogic signal $S_L(t)$:

$$S_L(t) = \alpha U(t) \tag{8}$$

where $\alpha$ is a calibration constant.

By assuming that $u(t) \ll U(t)$, it is possible to show [24] that

$$\overline{C} = C_p\sqrt{\alpha}\frac{\overline{S}_{pp}}{b\sqrt{\alpha} + a\sqrt{\overline{S}_L}} \tag{9}$$

and

$$c(t) = \frac{\overline{C}}{\overline{S}_c}[(S_{pp} - \overline{S}_{pp}) - A(S_L - \overline{S}_L)] \tag{10}$$

with

$$A = a\frac{\overline{S}_{pp}}{2b\sqrt{\alpha\overline{S}_L} + 2a\overline{S}_L} \tag{11}$$

Figure 1 defines some parameters, while the experimental apparatus and measurement devices are presented in Figure 2.

The instantaneous signals $S_L(t)$ and $S_{pp}(t)$ were sampled following the Shannon criterion prior to storage in a signal analyser disc unit. Data processing was performed at the end of each run and generated, the fluctuations $c(t)$ and $u(t)$ by use of Relationships 10 and 12:

$$u(t) = \frac{S_L(t) - \overline{S}_L}{\alpha} \tag{12}$$

The probability density function, its first four statistical moments and power spectral densities were obtained by the fast Fourier transform (FFT) of the signals.

### 2.2. *Measurement techniques*

#### 2.2.1. *Convection velocity measurement*

The convection velocity of turbulent eddies was measured using the following procedure. The electrochemical probe measuring volume was positioned 8 mm downstream from that of the L.D.A. measuring volume. To avoid any side-effect of the concentration, a solution identical to that of the coflowing stream was injected during the operation. The L.D.A. and the electrochemical probe generate signals related to the velocity. The time delay, $\tau$, determined from the cross-correlation curves relative to these signals, allowed calculation of the convection velocity $V_c = \delta/\tau$ where $\delta = 8$ mm is the optimum distance between the two measuring volumes [24].

#### 2.2.2. *Determination of the axial velocity–concentration cross-correlation coefficient*

The determination of the axial velocity–concentration cross-correlation coefficient is based on the same procedure; however, in this case the distance $\delta$ is equal to 0.6 mm as recommended by [24].

## 3. Results

### 3.1. *Mean quantities $U^*$, $U_a^*$, $C^*$, $C_a^*$ and $V_c$*

To determine the turbulent Schmidt number $(Sc)_t = \nu_t/D_t$ of a jet flow conveying a scalar quantity like concentration, most authors use a half-width radius $h$ defined in the general case by

$$\frac{\overline{G}(X,h) - G_p}{\overline{G}_a(X,o) - G_p} = 0.5 \tag{13}$$

When the velocity and concentration profiles are similar, the ratio of the half width radii respectively relative to momentum $h_u$ and to concentration $h_c$ is directly related to the turbulent Schmidt number [17] by

$$(Sc)_t = (h_u/h_c)^2 \tag{14}$$

However, in the present paper, it is used for comparison purposes only.

The radial variation of the dimensionless axial mean velocity profiles $U^*$ and mean concentration profiles $C^*$ are similar from $X = 20d$. Their approximation by a Gaussian curve is perfectly acceptable; the approximation becomes better with an increase in $X$. It must also be noticed that the radial dispersion of the scalar quantity is more important (Figure 3). This is in agreement with a classical literature result [17]. The virtual jet origin, $X_o$, is defined as

$$G_a^* = \frac{\overline{G}_a(X) - G_p}{G_j - G_p} = K\left(\frac{d}{X - X_o}\right) \tag{15}$$

where $K$ is a constant. It means that the dimensionless quantity, $U_a^*$ and $C_a^*$, are inversely proportional to the abscissa $X$. Using $U_a^*$ or $C_a^*$, it is obtained $X_o = 6d$ for $m = 0.12$. This value is within the limits of results given in the literature ($X_0 = 0d$ [18], $X_0 = 2d$ [8], $X_0 = 7d$ [3] and Hinze [1] proposed $4d + md$). The radial variation of the axial mean velocity reveals a decrease in the velocity with an increase of $X$ near the axis (Figure 4). Furthermore, the radial coordinate of the inflexion point increases with $X$. The radial variation of the axial mean velocity for different values of the ratio $m = U_p/U_j$ is reported on Figure 5. On the axis $\overline{U}$ is almost multiplied by 2 when $m$ increases from 0.24 to 0.37. Such a result confirms those reported by Schetz [2] indicating a variation of $\overline{U}_a$ with either $m$ or the abscissa $X$. For $X = 20d$ and $m = 0.12$, the ratio of the convection velocity to the local mean velocity $V_c/\overline{U}$ is equal to 0.62 on the jet axis reaching 1.30 on the edge (Figure 6). For $X = 30d$, the value of the ratio is the same on the jet axis and does not exceed 1.20 on the edge. However, the obtained values are smaller than those (0.90 on the jet axis and 1.70 on its edge) reported by Wygnanski and Fiedler [3], who used an external quiescent fluid ($m = 0$).

### 3.2. *Fluctuating quantities ($u^*$, $c^*$), integral scales ($L_u$, $L_c$) and velocity–concentration cross-correlation coefficient ($R_{uc}$)*

Contrary to dimensionless axial mean velocity or mean concentration profiles, $u^*$ against $r/X$ profiles are not self-similar for values of $X$ less than $30d$ (Figure 7); the similarity is reached when $X > 51d$ (Figure 8). Furthermore, $u^*$ approaches a limit of 0.34 on the jet axis when $m = 0.11$. This value can be compared with the literature results as shown in Table 2. Moreover, the comparison of $u^*$ and $c^*$ profiles (Figure 8) shows the slightly faster radial dispersion of a passive contaminant with respect

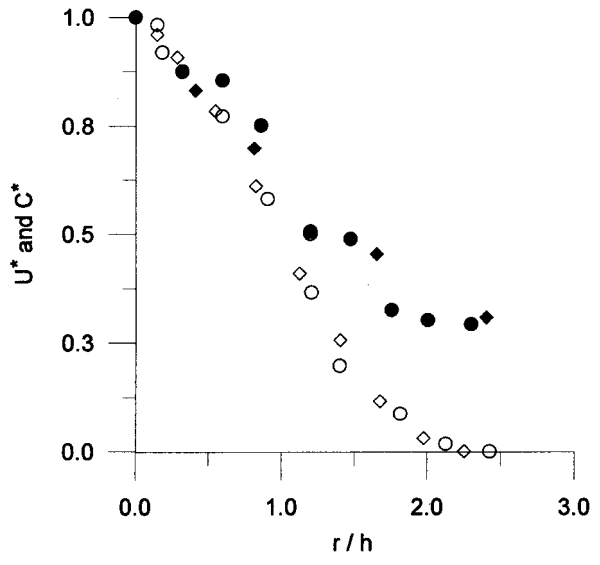


*Fig. 3.* Radial evolution of dimensionless axial mean velocity and mean concentration. Key: (○) $X = 51d$, $m = 0.11$, mean velocity; (◆) $X = 51d$, $m = 0$, mean concentratoin; (◇) $X = 57d$, $m = 0.11$, mean velocity; (●) $X = 57d$, $m = 0.11$, mean concentration.

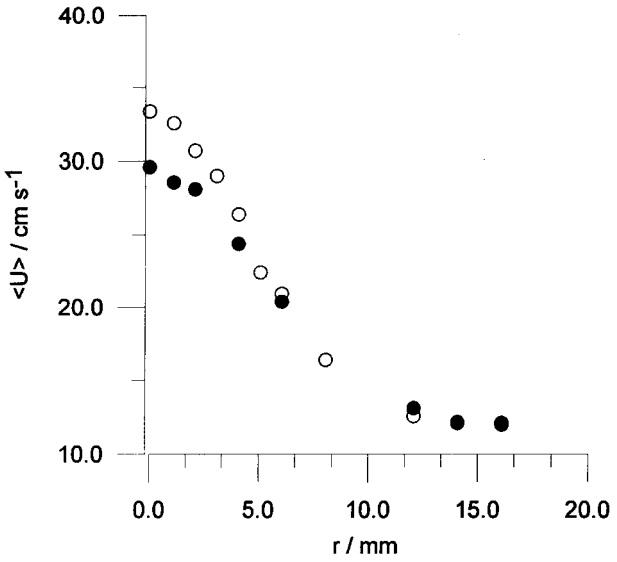


*Fig. 4.* Variation of the axial mean velocity with respect to the radius $r$ and to the abscissa $X$. $m = 0.12$. Key: (○) $X = 20d$ and (●) $X = 30d$.

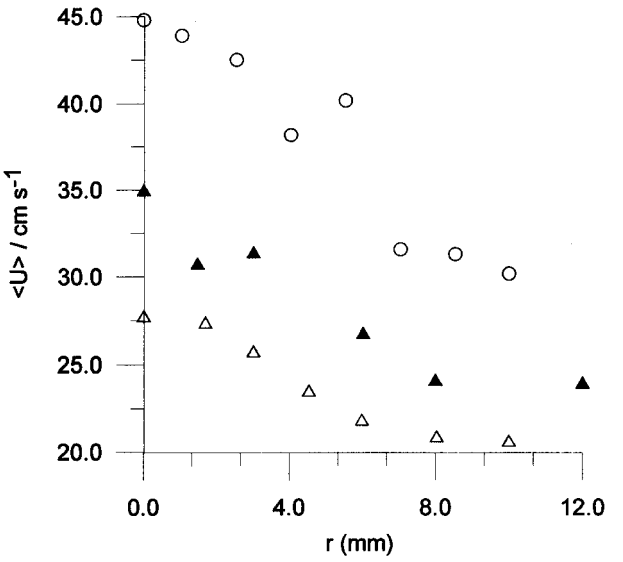


*Fig. 5.* Axial mean velocity profiles with respect to the velocities ratio $m$. $X = 25d$; $U_j = 84$ cm s$^{-1}$. Key: (△) $m = 0.24$, (▲) $m = 0.28$ and (○) $m = 0.37$.

to velocity. This result confirms to one obtained with the mean quantities (Figure 3).

The integral scale, $L_u$, relative to the axial velocity fluctuation $u(t)$ is determined by the Eulerian time correlation, given by

$$L_u = V_c \int_0^\infty R_E \, dt \tag{16}$$

with

$$R_E(\tau) = \frac{\overline{u(t)} \times \overline{u(t-\tau)}}{\overline{u^2}} \tag{17}$$

This scale slightly increases in the direction of the flow (Figure 9). On the jet axis, its value is approximately

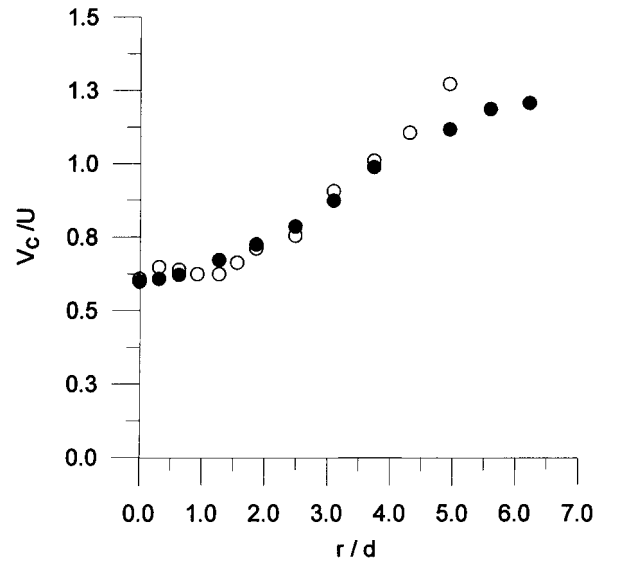


*Fig. 6.* Evolution of the convection velocity to the mean local velocity ratio through the jet. $m = 0.12$. Key: (○) $X = 20d$ and (●) $X = 30d$.

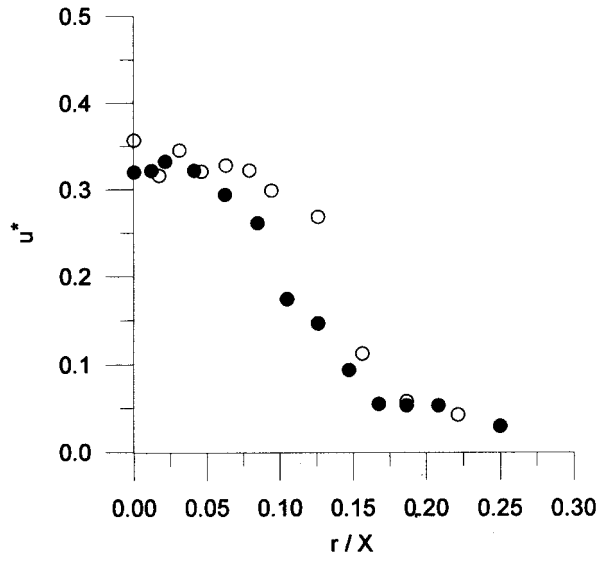


*Fig. 7.* Variation of axial velocity dimensionless r.m.s. through the jet. $m = 0.12$. Key: (○) $X = 20d$ and (●) $X = 30d$.

2.6$d$. The radial evolution of the axial velocity integral scale $L_u$ is the same for both $X$-values (Figure 9). A slight decrease of $L_u$ for small $r$ values is followed by a significant increase on the jet edge and a final sharp decrease when the coflowing stream is reached. It can also be noticed that $L_u$ does not exceed 3$d$ on the jet edge subjected, according to [3], to a high intermittency level. The value obtained on the axis is closer to that obtained, $L_u = 1.96d$, by Wygnanski and Fiedler [3] than the value of 1.36$d$ proposed by Antonia and Bilger [15].

The same procedure applied to the scalar concentration allows to define an integral scale by

$$L_c = V_c \int_0^\infty K_E \, dt \tag{18}$$

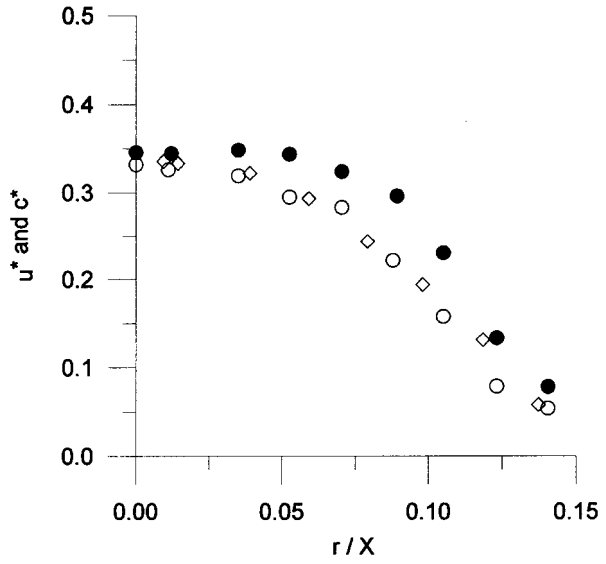


*Fig. 8.* Comparison of dimensionless axial velocity and concentration r.m.s. $m = 0.11$. Key: (○) $u^*$, $X = 57d$; (◇) $u^*$, $X = 51d$; (●) $c^*$, $X = 57d$.

*Table 2.* Comparison with the literature data of $u^*$ limit value

| Limit of $u^*$ | Authors | Value of $m$ | Value of $X/d$ |
|---|---|---|---|
| 0.47 | Antonia and Bilger [15] | 0.333 | 152 |
| 0.42 | Antonia and Bilger [15] | 0.222 | 266 |
| 0.40 | Siragna [11] | 0.44 | 33.4 |
| 0.38 | Siragna [11] | 0.24 | 24.1 |
| 0.34 | Present work | 0.11 | >51 |
| 0.283 | Nickels [6] | 0.091 | 90 |
| 0.28 | Wygnanski and Fiedler [3] | 0 | >40 |
| 0.274 | Nickels [6] | 0.333 | 90 |
| 0.25 | Tong and Warhaft [7] | 0 | 25 |
| 0.24 | Chevray and Tutu [10] | / | 15 |

where

$$K_E(\tau) = \frac{\overline{c(t)} \times \overline{c(t-\tau)}}{\overline{c^2}} \tag{19}$$

The radial evolution of the concentration integral scale is similar for $X = 51d$ and $X = 57d$, and $L_c = 1.78d$ on the jet axis (Figure 10). Shaughnessy and Morton [16], who performed their experiments with a Reynolds number 25 times greater than the one in the present work, have found a slightly higher value equal to $2.24d$. The difference between $L_c$ and $L_u$ corroborates the fact that the concentration field is relatively more dispersive compared to the velocity field.

Mixing is governed by the cross-correlation coefficient $R_{uc}$, defined by

$$R_{uc} = \frac{\overline{uc}}{\sqrt{\overline{u^2}} \times \sqrt{(\overline{c^2})}} \tag{20}$$

and calculated from the cross-correlation curves which have been obtained by using reverse FFT of the interspectra. On the jet axis, $R_{uc}$ is equal to 0.25 when $m = 0.11$ and the abscissa $X > 50d$ (Figure 11).

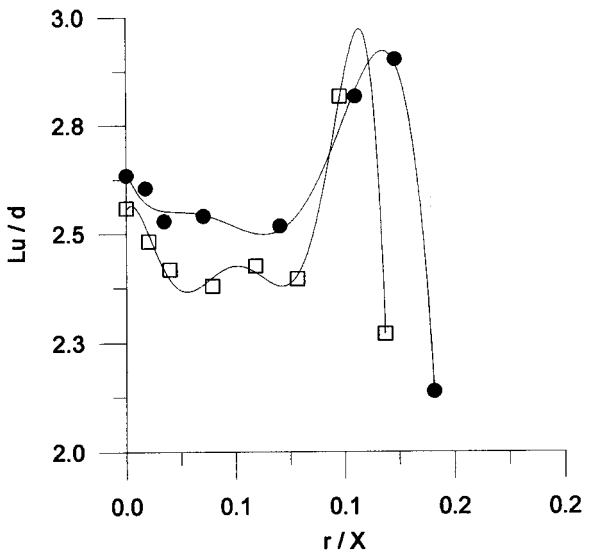


*Fig. 9.* Evolution of axial velocity integral scale through the jet. $m = 0.11$. Key: (□) $X = 51d$ and (●) $X = 57d$.

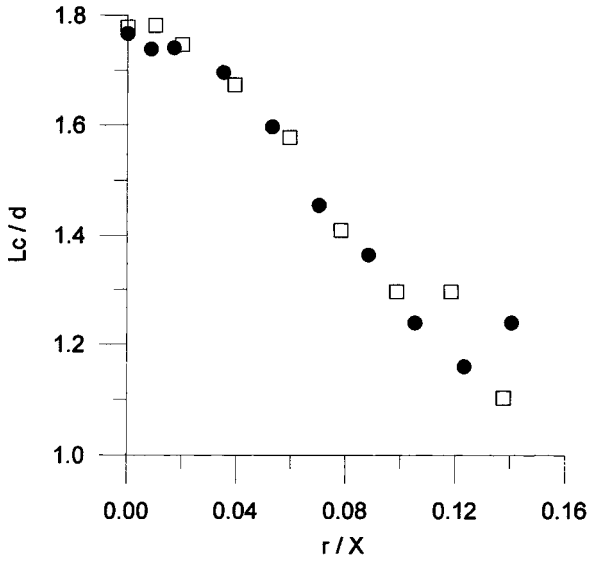


*Fig. 10.* Radial variation of the concentration integral scale through the jet. $m = 0.11$. Key: (□) $X = 51d$ and (●) $X = 57d$.

Maximum turbulent diffusion takes place near the jet edge where $R_{uc}$ reaches a maximum value of 0.50. This value, which seems to be a limit, was also obtained at $X = 15d$ by Chevray and Tutu [11] in the case of $R_{ut^\circ}$. It should be observed that the higher the turbulent diffusion and consequently $R_{uc}$, the better the mixing.

## 4. Conclusion

It is shown that the ratio of the turbulent eddy convection velocity to the local mean velocity may attain a value of 1.3; this value may affect the design of reactors. Furthermore, the results demonstrate the possibility of coupling L.D.A. to the polarographic

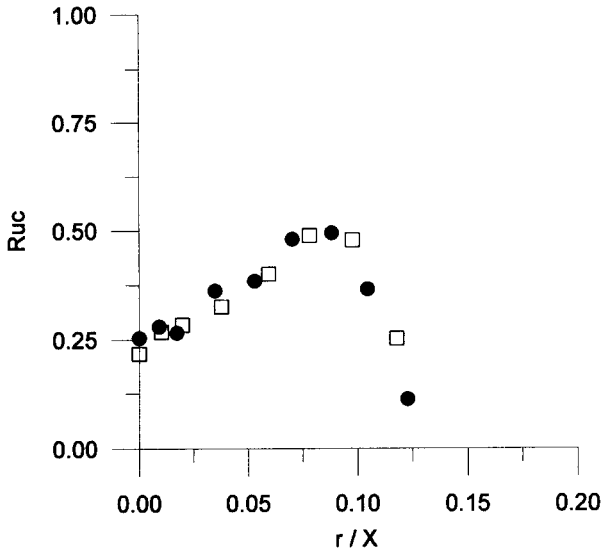


*Fig. 11.* Evolution of the axial velocity–concentration cross-correlation coefficient through the jet. $m = 0.11$. Key: (□) $X = 51d$ and (●) $X = 57d$.

technique for the determination of the velocity–concentration correlations in turbulent flows at relatively low Reynolds number.

## References


1. J.O. Hinze, 'Turbulence' (McGraw-Hill, 1975).
2. J.A. Schetz, 'Injection and mixing in Turbulent Flow, Progress in Astronautics and Aeronautics,' Vol. 68, edited by M. Summerfield (1980).
3. I. Wygnanski and H. Fiedler, *J. Fluid. Mech.* **38** (1969) 577.
4. D.R. Dowling and P.E. Dimotakis, *J. Fluid Mech.* **218** (1990) 109.
5. P.L. Miller and P.E. Dimotakis, *Phys. Fluids A* **3** (May 1991) 1156.
6. T.B. Nickels and A.E. Perry, *J. Fluid Mech.* **309** (1996) 157.
7. C. Tong and Z. Warhaft, *J. Fluid Mech.* **292** (1995) 1.
8. P.E. Miller and P.E. Dimotakis, *J. Fluid Mech.* **308** (1996) 129.
9. F. Lemoine, M. Wolff and M. Lebouché, *Experiments in Fluids* **20** (1996) 178.
10. F. Lemoine, Y. Antoine, M. Wolff and M. Lebouché, *C. R. Acad. Sci. Paris*, **325** (Sér. II) (1997) 511.
11. R. Chevray and N.K. Tutu, *J. Fluid Mech.* **88** (1978) 133.
12. S. Benayad, R. David and G. Cognet, *Chem. Eng. Process.* **19** (1985) 157.
13. J.M. Gatard, Thése de Doctorat 3éme Cycle, Université de Poitiers, France (1980).
14. P. Siragna, Thése de Doctorat d'Ingénieur, I.N.P.L. Nancy, France (1982).
15. R.A. Antonia and R.W. Bilger, *J. Fluid. Mech.* **61** (1973) 805.
16. E.J. Shaughnessy and J.B. Morton, *J. Fluid Mech.* **80** (1977) 129.
17. G.N. Abramovich, 'The Theory of Turbulent Jets' (MIT Press, 1963).
18. W. Forstal and E.W. Gaylord, *J. Appl. Mech.* (1955) 161.
19. P. Chassaing and A. Claria, *Int. J. Heat Mass Transf.* **19** (1976) 249.
20. A. Birch, D. Brown, M. Dodson and J. Thomas, *J. Fluid. Mech.* **88** (1973) 431.
21. H. Wu and G.K. Patterson, *Chem. Eng. Sci.* **44** (1989) 2207.
22. S. Michelet, A. Kemoun, J. Mallet and M. Mahouast, *Experiments in Fluids* **23** (1997) 418.
23. R.A. Antonia, A.J. Chambers and A.K.M.F. Hussein, *Phys. Fluids* **23** (1980) 871.
24. S. Benayad, Thése de Doctorat de 3éme Cycle, I.N.P.L. Nancy, France (1984).
25. F. Durst and J.H. Whitelaw, 'Principles and Practice of Laser Doppler Anemometry', (Academic Press, 1976).